Chem Biol Drug Des 2012; **79:** 223–234

doi: 10.1111/j.1747-0285.2011.01265.x

Research Letter

Synthesis of Oxovanadium(IV) Schiff base Complexes derived from C-substituted Diamines and Pyridoxal-5-Phosphate as Antitumor Agents

Puja Panwar Hazari[1,*], Anand Kumar Pandey[1,2], Shubhra Chaturvedi[1], Anjani Kumar Tiwari[1], Sudhir Chandna[3], Bilikere Srinivasarao Dwarakanath[3] and Anil Kumar Mishra[1,*]

[1]Division of Cyclotron and Radiopharmaceutical Sciences, Institute of Nuclear Medicine and Allied Sciences, Brig SK Mazumdar Road, New Delhi 110054, India
[2]School of Biomedical Engineeering, Institute of Technology, Banaras Hindu University, Varanasi 221005, Uttar pradesh, India
[3]Division of Radiation Biosciences, Institute of Nuclear Medicine and Allied Sciences, Brig SK Mazumdar Road, New Delhi 110054, India
**Corresponding authors: Anil Kumar Mishra, akmishra@inmas.drdo.in, Puja Panwar Hazari, puja_panwar@yahoo.com*

Oxovanadium (IV) complexes of *N,N*′-bispyridoxyl-5, 5′-bis (phosphate) ethylenediimine (L1) and *N,N*′-bis(pyridoxyl)-5,5′-bis(phosphate)-1′′-(*p*-nitrobenzyl)ethylenediimine (L2) were synthesized by condensation of optically active C-substituted diamines and pyridoxal-5-phosphate. Oxovanadium (IV) complexes derived from L1 and L2 were evaluated as DNA cleavage agent (cleavage of supercoiled plasmid pBR322 DNA). Interestingly, both the oxovanadium (IV) complexes exhibited DNA nuclease activity, and the extent of oxidation of DNA by these vanadyl complexes was superior to $VOSO_4$. The significant reduction in primary tumor and increased delay in tumor growth of 15 days was seen in the tumor regression analysis with oxovanadium (IV) complex of L1. With the preliminary studies performed with the pyridoxal-5-phosphate -based salen derivatives including the cytotoxicity and tumor regression, it is evident that the salen bifunctional chelating agent has obtained therapeutic potential if conjugated to a gene-specific targeting molecule for the oxidation of guanine residue.

Key words: bifunctional chelating agent, chemical nucleases, cytotoxicity, DNA modification, pyridoxal-5-phosphate, Schiff base, vanadium complex

Abbreviations: [VO-(L1)], *N,N*′-bispyridoxyl-5,5′-bis (phosphate) ethylenediimine vanadium complex; [VO-(L2)], *N,N*′-bis(pyridoxyl)-5,5′-bis(phosphate)-1-(*p*-nitrobenzyl)ethylenediimine vanadium complex; P-5-P, pyridoxal-5-phosphate; ROS, reactive oxygen species; BFC, bifunctional chelating agent; U-87MG, U-87 malignant glioma; MTT, 3-(4,5-dimethylthiazole-2-yl)-2,5-diphenyl-2H-tetrazolium bromide; MPE, β-mercaptoethanol.

Received 16 December 2010, revised 26 July 2011 and accepted for publication 2 October 2011

Current efforts are on to design transition metal complexes based on vanadium that can act as chemical nucleases suitable for plasmid nicking or in a direct strand scission of the genomic DNA. Potential Schiff base ligands derived from condensation reaction of ethylenediamine with aldehyde group of pyridoxal-5-phosphate have been prepared, and its oxovanadium complexes were investigated for DNA cleaving activity. The preparation of early-transition metal complexes with chelating ligands, such as derivatives of Schiff base salen{bis(salicylidene)imino}V=O complex, has been reported in literature (1,2). Antimicrobial/antitumor/cytotoxic activities of vanadium (IV), manganese (IV), iron (III), cobalt (II), and copper (II) complexes have also been reported (3–6). These complexes are air stable, good Lewis acids, and have been previously employed as asymmetric catalysts. Vanadium is a transition element that exists in several oxidation states, including +2, +3, +4, and +5. Only the +3, +4, and +5 oxidation states are important in biological systems (7–11). Several organometallic complexes of vanadium exhibit antitumor properties both *in vitro* and *in vivo*, primarily via oxidative damage (12,13). Vanadium compounds induce cell cycle arrest and cytotoxic effects through DNA cleavage and plasma membrane lipoperoxidation (14,15). Vanadium may also exert inhibitory effects on cancer cell metastases potentially through modulation of cellular adhesive molecules, and reverse antineoplastic drug resistance. Redox-active transition metal complexes in the presence of oxidants have been extensively used for DNA cleavage reactions (16). In a typical reaction, an oxidizing agent like O_2, H_2O_2, or a peracid is added in addition to the transition metal complex (17).

Previously, pyridoxal-based chelators have shown antitumor activity when bound to metal ion; for instance, pyridoxal isonicotinoyl hydrazone (PIH) compounds have a high affinity and specificity for Fe(III), and some of its analogs have been shown to possess marked Fe chelation efficacy in a wide variety of biological systems both *in vitro* and *in vivo*. Antineoplastic activity of these ligands based on PIH has been reported in literature (18). Attachment of the chelating agents to the biologically active molecule is readily accomplished because of the functionalization of the ligand *N,N*′-bis(pyridoxyl)-5,5′-bis(phosphate)-1′′-(*p*-nitrobenzyl)ethylenediimine (L2) derived from optically active amino acid. There is significant interest in the

synthesis and properties of Schiff bases bearing pendant arms, and their transition metal complexes have an application as antitumor agents.

In an systemic effort to identify a potent anticancer agent, we synthesized oxovanadium (IV) complexes of *N,N′*-bispyridoxyl-5, 5′-bis (phosphate) ethylenediimine (L1) and *N,N′*-bis(pyridoxyl)-5,5′-bis(phosphate)-1′′-(*p*-nitrobenzyl)ethylenediimine (L2) and examined their cytotoxic activity against two different human cancer cell lines [U-87 malignant glioma (U-87MG) and MDA-MB-468)]. The Schiff base ligand and its oxovanadium (IV) complex were synthesized based on the previously published chemistry. The studies, including the cytotoxicity and tumor regression, performed with the pyridoxal-5-phosphate (P-5-P)-based derivatives indicate that these agents have obtained therapeutic potential against tumors of human origin.

Materials and Methods

Pyridoxal-5-phosphate monohydrate and vanadyl sulfate trihydrate salt were obtained from Fluka. The corresponding diamine derivative (**2a**) of optically active amino acid was synthesized in our laboratory by the standard procedure (19). Salicylaldehyde, sodium borohydride, stannous chloride dihydrate, and other solvents (Sigma-Aldrich Co., St. Louis, MO, USA) were used as received. TLC was run on plastic-backed silica gel plates (0.2-mm-thick silica gel 60 F-254; E. Merck, KGaA, Darmstadt, Germany) using a 10% w/v aqueous ammonium acetate/CH_3OH (1:1 v/v) solution as eluant.

MDA-MB-468 kindly provided by Dr Normando, (CIMAB SA, Havana) and human malignant glioma cells, U-87MG (NCCS, Pune, India), were maintained at 37 °C in a humidified CO_2 incubator (5% CO_2, 95% air) in DMEM (Sigma-Aldrich Co.) supplemented with 10% fetal calf serum (Biological industries, Kibbutz Beit Haemek, Israel), 50 U/mL penicillin, 50 μg/mL streptomycin sulfate, and 2 μg/mL nystatin. Cells were routinely subcultured twice a week using 0.05% Trypsin (Sigma) in 0.02% EDTA.

The ^{1}H NMR spectra were determined by using Bruker Spectro spin 400 MHz at INMAS, Delhi. The ^{31}P NMR spectra were determined by using Bruker Spectro spin 400 MHz at INMAS, Delhi. The decoupled spectra were recorded with the decoupling frequency matching that of proton. Mass spectrum was recorded on a JEOL SX 102/DA-6000 Mass spectrometer using m-nitrobenzyl alcohol as the matrix (Agilent 1100, Karlsrhue, Germany, and Thermofisher, Bombay India). Animal protocols have been approved by Institutional Animal ethics Committee. New Zealand Rabbits and albino BALB/c mice were used for blood clearance, imaging, and biodistribution. Mice and rabbits were housed under the conditions of controlled temperature of 22 ± 2 °C and normal diet.

Cell cycle distribution was studied with the help of FACS Caliber (Becton-Dickinson & Co., Mountain View, CA, USA) flow cytometer using the CELL QUEST (version 3.0.1; Becton Dickinson and Co.) and Mod fit L T (version 2.0 software House, Inc, Becton Dickinson and Co.) software for acquisition and analysis, and a minimum of 10 000 cells per sample were analyzed.

Statistical methods

Data are reported as mean ± standard deviation (SD/SE). One-way ANOVA analysis was carried out to determine whether there is a statistically significant difference between combinations used to evaluate the synergistic effect.

Synthesis of oxovanadium (IV) complex of *N,N′*-bispyridoxyl-5, 5′-bis (phosphate) ethylenediimine (1b)

Synthesis of N,N′-bispyridoxyl-5, 5′–bis (phosphate) ethylenediimine [L1] (**1a**). A solution of pyridoxal-5-phosphate monohydrate (0.25 g; 0.94 mmol) in 10 mL methanol was stirred, and when a homogeneous solution was obtained, 30 μL of ethylenediamine (0.44 mmol) was added. A bright yellow precipitate of the bis(imine) was formed immediately (Scheme 1). The reaction mixture was allowed to stir over night at 18–20 °C, and the precipitate was filtered, washed with methanol, and dried under vacuum. Yield 72% ^{1}H NMR (400 MHz, D_2O pH 8) 8.97 (Ar, 1H, s), 7.68 (Ar, 1H, s), 5.09 (2H, m), 2.4 (4H, s). ^{13}C NMR (100 MHz, D_2O pH 8) 162.8, 153.1, 145.2, 144.7, 140.9, 131.4, 61.9, 29.6, 14.9. ESI-MS Found 517.2 $[M\text{-}H]^+$; Calcd m/e 518.35. Elemental Anal. Calcd for $C_{18}H_{24}N_4O_{10}P_2$ C, 41.71; H, 4.67; N, 10.81. Found : C, 41.70; H, 4.68; N, 10.83.

Synthesis of oxovanadium (IV) complex of *N,N′*-bispyridoxyl-5, 5′-bis (phosphate) ethylenediimine [VO-(L1)] (1b)

To a hot methanol solution (20 mL) of vanadyl sulfate (0.347 g, 0.193 mmol) was added the ligand *N,N′*-bispyridoxyl-5, 5′-bis (phosphate) ethylenediimine (0.100 g, 0.193 mmol) and pyridine (0.35 mL, 0.34 g, 4.34 mmol), and the mixture was stirred for 1 h at 60 °C. The

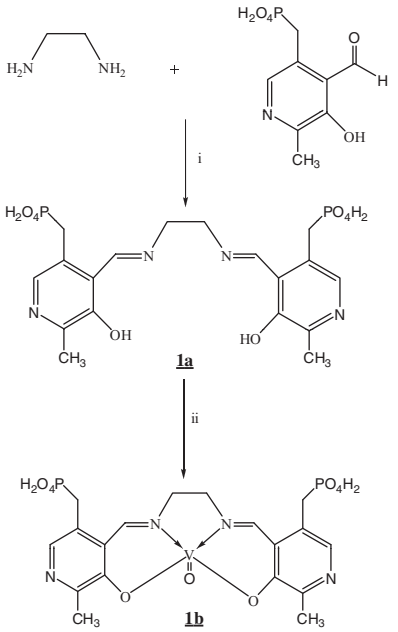

Scheme 1: Synthesis of oxovanadium (IV) complex of *N,N′*-bispyridoxyl-5, 5′-bis (phosphate) ethylenediimine. Reagents (i) methanol (ii) $VOSO_4$/pyridine.

suspension was then kept at room temperature, and the resulting green precipitate was collected by filtration and washed thoroughly with water, methanol, and diethyl ether. Yield 84% calc., IR(KBr) ν, /cm 3401, 2921, C=N stretch was observed at 1637/cm, 1591,1508, 1424, 1387, 991,V-O (614/cm), 495, V-N (466/cm) ESI-MS: Found 585.3 $[M + 2H]^+$, Calcd for $C_{18}H_{22}N_4O_{11}P_2V$: m/e 583.28. ^{31}P NMR: (D_2O) 4.349 (br). Elemental Anal. Calcd for $C_{18}H_{22}N_4O_{11}P_2V$ C, 37.07; H, 3.80; N, 9.61 Found: C, 37.09; H, 3.83; N, 9.62.

Synthesis of *N,N′*-bis(pyridoxyl)-5,5′-bis(phosphate)-1″-(*p*-nitrobenzyl) ethylenediimine [L2] (2b)

p-Nitrobenzylethylenediamine (**2a**) was synthesized as reported previously (19). A solution of pyridoxal-5-phosphate monohydrate (0.598 g; 2.2 mmol) in 10 mL methanol was stirred, and when a homogeneous solution was obtained, 0.2 g of (**2a**) (1.02 mmol) was added. A bright yellow precipitate of the bis(imine) was formed immediately. The reaction mixture was allowed to stir over night at 18–20 °C. The precipitate was filtered, washed with methanol, and dried under vacuum. Yield 82% IR(KBr) ν, /cm 3398, C=N stretch; 1645, 1473, 1321, 1157, 1029, 825 734 590 ESI-MS: Found 654.80 $[M + H]^+$Calcd for $C_{25}H_{29}N_5O_{12}P_2$: m/e 653.14 ^1H NMR (400 MHz,D_2O) 8.90(Py-Ar,2H,s), 8.51–8.49 (Ar, 2H,d; J = 12Hz), 7.81–7.79 (Ar,2H, J = 12Hz), 7.58(2H, s), 3.4 (1H, t), 3.27(2H, s), 1.98(s). ^{13}C NMR (100 MHz, D_2O) 162.3, 145.6, 144.3, 134.2, 130.3, 122.2, 61.7, 56.7, 42.1, 28.9, 14.2. Elemental Anal. Calcd for $C_{25}H_{29}N_5O_{12}P_2$ C, 45.95; H, 4.47; N, 10.72; Found: C, 45.91; H, 4.44; N, 10.71.

Synthesis of oxovanadium (IV) complex of *N,N′*-bis(pyridoxyl)-5,5′-bis(phosphate)-1″-(*p*-nitrobenzyl)ethylenediimine [VO-(L2)] (2c)

To a hot methanol solution (20 mL) of vanadyl sulfate (0.026 g, 0.16 mmol), **2b** (0.1 g; 0.16 mmol) and pyridine (0.3 mL, 3.62 mmol) were added and the mixture was stirred for 1 h at 60°C. Yield 88% IR(KBr) ν, /cm 3395, 2089, C=N stretch; 1639, 1510, 1392, 1208, 1079, 987, 844, 722,621, V-N stretch; 467. ESI-MS: Found 721 $[M + 3H]^+$; Calcd for $C_{25}H_{27}N_5O_{12}P_2V$: m/e 718.(Scheme 2). Elemental Anal. Calcd. for $C_{23}H_{19}N_5O_{11}P_2V$; C, 43.75; H, 3.96; N, 10.20; Found: C, 43.76; H, 3.94; N, 10.22.

EPR measurements

EPR spectra were recorded on an X-band Bruker ER200D-SCR spectrometer. Measurements were recorded in fluid solution at 298 K (1 mM in H_2O/DMSO 80/20) and in frozen solution at 77 K with incident power sufficiently low (12 mW) to avoid saturation effects and a modulation frequency of 100 kHz. Modulation amplitudes from 1 to 10 G were used. The *g* values were determined by measuring the magnetic field, H, and the microwave frequency. 2,2-diphenyl-1-picrylhydrazyl is taken as standard.

MTT and clonogenic assays

The cytotoxicity of oxovanadium (IV) complexes was tested in human cancer cell lines using 3-(4,5-dimethylthiazole-2-yl)-2,5-diphenyl-2H-tetrazolium bromide (MTT) assay; 1×10^4 cells/well were plated in 200 μL of the complete medium, and treatment was given 24 h after plating. Cells were exposed continuously with varying concentrations of the complex (0.1–500 μM) in PBS in a volume of 50 μL, and MTT assays were performed at the end of fourth day. At the end of treatment, cells were incubated with MTT at a final concentration of 0.05 mg/mL (20 μL) for 2 h at 37 °C, and the medium was removed. The cells were lysed and the formazan crystals dissolved using 150 μL of DMSO. Optical density was measured at 570 with 630 nm as reference filter.

Macrocolony assay

Monolayer cultures of MDA-MB-468 and U-87MG cell lines were trypsinized, and 100–1000 cells were plated in 60-mm Petri dishes

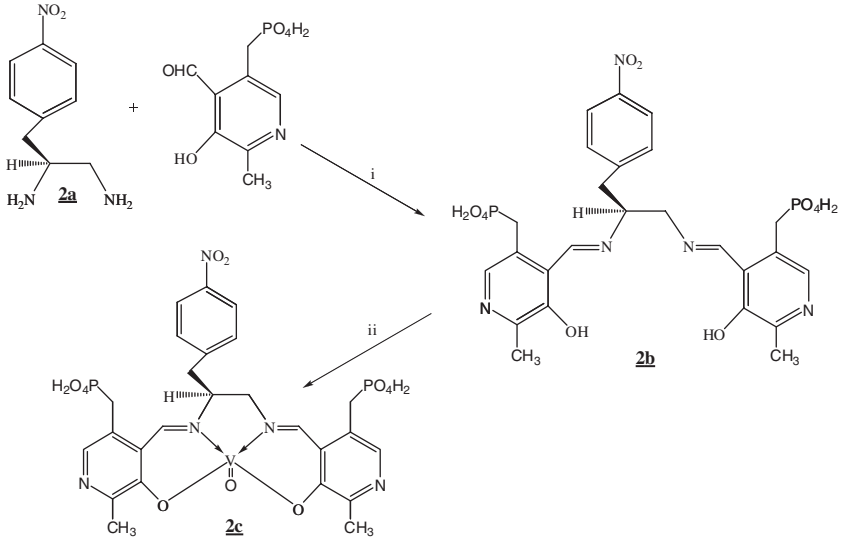

Scheme 2: Synthesis of oxovanadium complex of *N,N′*-bis(pyridoxyl)-5,5′-bis(phosphate)-1″-(*p*-nitrobenzyl)ethylenediimine. Reagents (i) methanol, pyridoxal-5-phosphate (ii)$VOSO_4$/pyridine.

depending on the concentrations of the complex and incubated at 37 °C in 5% CO_2 humidified atmosphere. Growth media were changed every third day. Colonies were fixed in methanol and stained with 1% crystal violet. Plating efficiency was calculated as P.E. (%) = No. of colonies/No. of cells plated × 100. Surviving fraction (SF) was calculated.

DNA cleaving experiments

Experiments with plasmid DNA pBR322 on agarose gels

Each reaction mixture contained 2 μL of supercoiled pLAZ DNA pBR322 (1 μg), 2 μL of Tris–HCl/NaCl 10 mM buffer at pH 7.0, 6 μL of water, and 10 μL of the [VO-(L1)] and [VO-(L2)] compound at the desired concentration (0.1 and 0.25 mM) that were prepared in 100% PBS immediately before use. After 2-h incubation at 37 °C or overnight at room temperature, 5 μL of loading buffer (0.25% bromophenol blue, 0.25% xylene cyanol, and 30% glycerol in water) was added to each tube and the solution was loaded onto 1% agarose gel. The electrophoresis was carried out for about 2 h at 120 V in TAE buffer (89 mM Tris–acetate, 1 mM EDTA, pH 8.3). Gels were stained with ethidium bromide (11 g/mL) and destained with water prior to being photography of following UVA excitation of 360 nM.

Cell cycle analysis

Exponentially growing cells were incubated with 0.1 mM of oxovanadium compounds for 24 h at 37 °C. Cells were harvested by trypsin release and resuspended in DNA staining solution (10 μg/mL RNAse, 0.1% Triton X-100, 0.1 mM EDTA, 0.1% sodium citrate, 50 μg/mL PI, and 1 mM Tris–HCl) 1–2 h prior to flow cytometric analysis. The fluorescence of 10 000 cells was measured using flow cytometer (Facscalibur; Becton Dickinson) with excitation of 488 nm. The percentage of cells in G_1, S, and G_2-M was determined by analyzing the DNA histograms with modfit software provided by the manufacturer.

Tumor regression analysis

Seven-week-old female BALB/c mice (n = 10, weight = 28–30 g) received a subcutaneous injection of 10^5 Ehrlich ascites tumor (EAT) cells on the right hind leg. Complex was administered via i.v. injections. The study began treatment after tumor volume has reached 0.5–0.7 cm^3. [VO-(L1)] treatment was given in volume of 100 μL at 400 mg/kg of dose every 48 h beginning on day one and continuing for 10 doses. The mice were weighed once a week throughout the trial. The day of tumor detection was recorded, and the dimensions of the tumors were measured every 48 h. As life span was one of the parameters considered in the study, the mice were brought to survival approximately 2–3 days before their natural death. The tumor development study lasted 40 days.

Results

Spectroscopic characterization

The ligand *N,N′*-bispyridoxyl-5, 5′-bis (phosphate) ethylenediimine and C-substituted diimine form stable water-soluble chelates involving the P-5-P hydroxy groups (Schemes 1 and 2). Both ligands were easily synthesized in high yield and were characterized by IR, elemental analyses, mass, and NMR spectroscopy. Signal for (V-N) stretch was observed for [VO-(L1)] and [VO-(L2)] in the region at 466 and 467/cm, respectively, and ν (V-O) stretching for [VO-(L1)] occurred at 614/cm as reported for other oxovanadium derivatives (20). P-NMR chemical shifts are independent of formal oxidation numbers. Rather, they depend on the actual electron density on phosphorous, the bond angles, and pi-bonding. After complexation, ^{31}P-NMR of the complex shows a downfield change in chemical shift, which confirms the metal complexation. The elemental analyses demonstrate the stoichiometric relation of atoms in the compounds. The molecular ion peak (ESI-MS) at 585.3 and 721 for [VO-(L1)] (Figure 1) and [VO-(L2)] (Figure 2) reflects that there is no solvent bounded in the axial position of the ligand.

Figure 3 shows the EPR spectrum of the compound [VO-(L1)] and [VO-(L2)]. The spectra were recorded at 293 K and found to consist of eight well-resolved hyperfine splitting lines, which were not equivalent in intensity. The G and A values obtained in the spectra give an idea of the environment around V(IV): g is 1.972 and A is

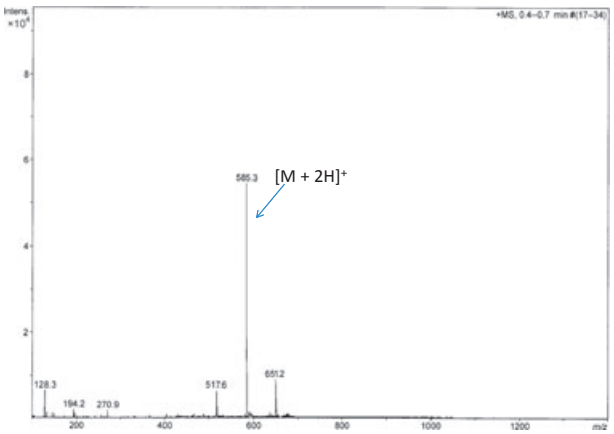

Figure 1: Mass spectrum of oxovanadium (IV) complex of *N,N′*-bispyridoxyl-5, 5′-bis (phosphate) ethylenediimine [VO-(L1)].

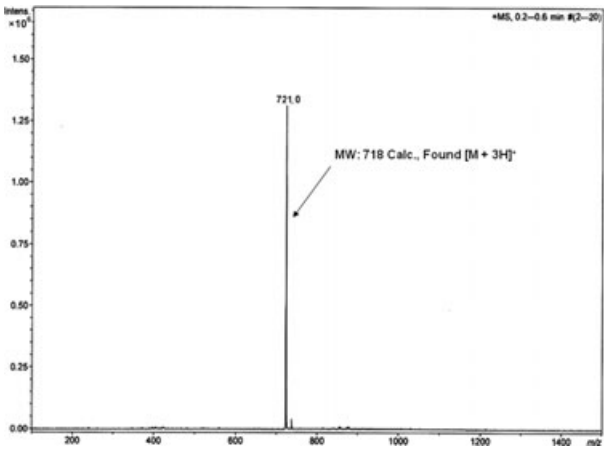

Figure 2: Mass spectrum of oxovanadium (IV) complex of *N,N′*-bis(pyridoxyl)-5,5′-bis(phosphate)-1-(*p*-nitrobenzyl)ethylenediimine [VO(L2)].

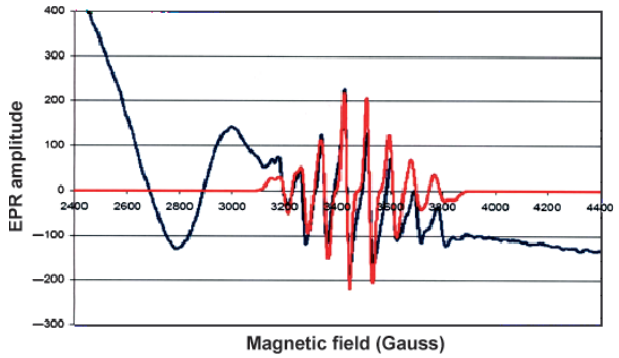

Figure 3: EPR spectrum of VO-L1 (red) and VO-L2 (blue) recorded at 293 K in H_2O/DMSO (80/20).

Table 1: Potentiometric species distribution pattern of $VOSO_4$, [VO-(L1)] system in the presence and absence of oxidant and reductant

pH	VO2+	V(III)	V(IV)	V(V)
	$VOSO_4$	β-mercaptoethanol	–	$NaIO_4$
1	92	0	7.6	2
2	72.3	5	11	3
3	70.4	5.9	17.7	5
4	30.6	7.6	23.5	5
5	18.1	6.5	40	6
6	10.2	0.6	33	0.8
7	5.1	0.5	30	0.8
8	3.2	0.5	29	1
9	3.1	0.4	25	1
10	2.9	8.5	21	6
11	2.7	7	11	11
12	1.5	0	7	15
13	1.4	0	6	15.5
14	1.3	0	2	13

$\sim 85 \times 10^{-4}$/cm, $A/G^{\parallel} = 84$, GI = 1.972, $A^{\perp}/G = 94$ for [VO-(L1)], and for [VO-(L2)], g is 1.989 and A is 89×10^{-4}/cm, which indicated distorted octahedral symmetry. EPR data for [VO-(L1)] and [VO-(L2)] revealed that g values are close to 2 which are for the unpaired electron in a non-degenerate orbital. Any orbital angular momentum is subsequently quenched resulting in a 'spin-only' system. In addition, there should be little mixing in of an orbital component from excited states through spin–orbit coupling, leading to typical g values close to, but slightly less than, 2. Similar signals have been reported by Verquin *et al.* (20) for vanadium (IV).

Potentiometric speciation in aqueous solution

Potentiometric titration was carried out in aqueous solution to check the behavior in solution. The metal ligand system was described by the formation of [VO-(L1)] 1:1 species. The speciation in solution at different pH was obtained for $VOSO_4$, [VO-(L1)] in the presence of mercaptoethanol and $NaIO_4$. At physiological pH, the species distribution pattern of vanadium complexes in solution shows that only one species V(IV) exist as a major species, while at lower and higher pH, two species V(III) and V(V) were predominant, respectively, as seen in pH/species distribution Table 1. The evaluation of the titration of the [VO-(L1)] and [VO-(L2)] systems at 0.1 M ionic structure (25 °C) yielded the stability constants 16.4 and 17.2, respectively, when metal and ligand were taken in 1:1 ratio (1 mM each).

Plasmid DNA on agarose gel

We have investigated vanadium complexes capable of reacting with O_2 in the presence of a reductant to generate V(III) species leading to oxidative damage at guanine residue of DNA (G). With redox-active ligands, the role of V(III) is to trigger formation of ligand radicals capable of generating covalent adducts (17).

DNA cleavage was analyzed by monitoring the conversion of supercoiled plasmid DNA pBR322 (Sc) to nicked circular DNA (Nck) and linear DNA (Lin) (Figure 4). Under aerobic conditions, the [VO-L1] was able to trigger oxidative cleavage of DNA by 38% in the absence of any activating agent (Table 2).

Vanadium complexes caused molecular oxygen-dependent DNA strand break in cooperation with H_2O_2-generated OH radicals. Incubation of the plasmid with the vanadium complexes in the presence of H_2O_2 at 37 °C for 2 h or at rt for 24 h caused conversion of the Sc form to the Nck form. The cleavage reaction could be activated by the addition of either a reducing agent or an oxidant with the complex significantly promoting DNA cleavage in the presence of β-mercaptoethanol (MPE) (Figure 4B).

Modification of DNA by salen complexed with vanadyl ion was also studied in the presence of an oxygen donor compound, sodium periodate. In this case, plasmid DNA modification was much more effective than the reducing agent as complete conversion of Sc form to Nck 52% and Lin 47% forms was observed at 0.25 mM concentration. Indeed, in all the cases, the Sc form of the plasmid DNA was practically converted into the Nck and Lin forms (Figure 4). When the DNA was incubated for 2 h at 37 °C in the presence of oxidizing agent $NaIO_4$, it caused substantial DNA cleavage, and with complete conversion of the Sc form to the Nck and Lin DNA molecules (excess single-strand breaks enhance the probability of double-strand scissions). The DNA cleavage efficiency increased with the concentration of the redox agent (0.15 or 0.2 mM) as well as the complex (0.1, 0.25, 0.5 mM). It is also worth noting that all combinations and the complex alone exhibited nuclease activity. Similar results were obtained with the bifunctional oxovanadium complex as well. In this case, however, plasmid DNA cleavage was effective in the presence of both reducing and oxidizing agent. The Sc form of plasmid DNA was completely converted into the Nck (79%) and Lin (20%) forms. Presence of optically active p-NO_2-phenylalanine imparted cleavage with reducing agent by successful conversion into Nck and Lin forms at 0.1 mM, which was seen at 0.25 mM for VO-L1. This could be attributed to the presence of chiral center in VO-L2. Interestingly, 0.1 mM of the bifunctional oxovanadium complex with $NaIO_4$ in the presence of H_2O_2 completely digested DNA (Figure 4D).

Cytotoxicity studies of oxovanadium compounds against human tumor cell lines

[VO-(L1)] and [VO-(L2)] were tested for the ability to induce cytotoxicity in the cancer cell lines using both an assay of mitochondrial activ-

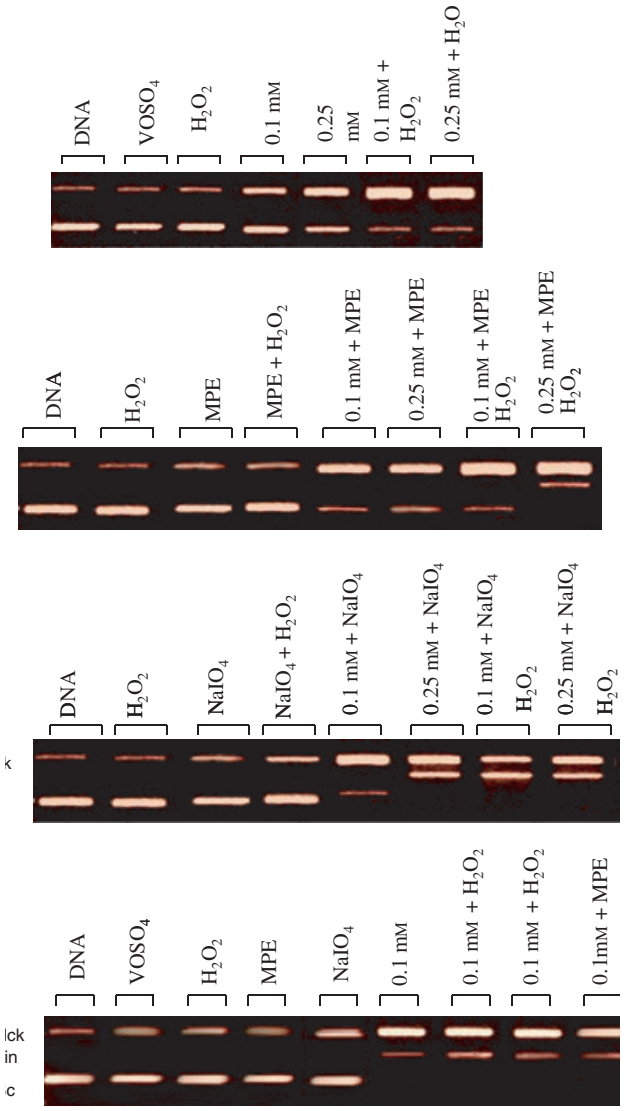

Figure 4: Cleavage of supercoiled plasmid DNA pBR322 (Sc) by [VO-(L1)] (0.1 and 0.25 mM): 3(A) in the presence of H_2O_2; 3(B) β-mercapotoethanol (MPE) as reducing agent; 3(C) $NaIO_4$ as oxidant; 3(D) nuclease activity of bifunctional [VO-(L2)] complex. The lanes marked DNA, H_2O_2, $VOSO_4$, MPE, $NaIO_4$, MPE + H_2O_2, and $NaIO_4$ + H_2O_2 refer to the plasmid DNA incubated without drug as controls. The DNA was incubated for 2 h at 37 °C.

ity (in a MTT assay) and a clonogenic survival. Both the vanadium complexes showed a concentration-dependent cytotoxicity in U-87MG cells (Figure 5). A known number of cells were treated with increasing concentration (0.1–500 μM) of [VO-(L1)] and [VO-(L2)] for 48 h in DMEM and the metabolic viability assayed. A concentration-dependent decrease in the fraction of the metabolically viable cells was observed with 40% decrease in viability at 0.5 mM (Figure 5). Twofold decrease was observed for the [VO-(L2)] as compared to the [VO-(L1)] complex.

U-87 malignant glioma cells were treated with minimal concentration, 0.01 μM of H_2O_2 (ED_{50} of H_2O_2 reported to be 50–100 μM), so as to suppress its oxidizing effect (14). The cytotoxic effects of activating agents, reductant (2-mercaptoethanol), and oxidant (sodium periodate) in combination with the complex were studied in the absence and presence of H_2O_2.

Treatment of cells with hydrogen peroxide (0.01 μM) and activating agents in the absence of complex did not induce marked cytotoxic

Table 2: Cleavage of supercoiled plasmid DNA (1 g) pBR322 (Sc) by [VO-(L1)] (**1b**) and [VO-(L2)] (**2c**) complexes incubated for 2 h at 37°C in the presence of H_2O_2, β-Mercaptoethanol (MPE) as reducing agent and $NaIO_4$ as an oxidant

	Drug		Reaction condition			DNA (form)		
S. no.	[VO-(L1)]	[VO-(L2)]	H_2O_2	MPE	$NaIPO_4$	Sc	Nck	Lin
1	–	–	–	–	–	82	18	–
2	–	–	0.01 μM	–	–	79	21	–
3	–	–	–	200 μg	–	72	28	–
4	–	–	–	–	200 μg	70	30	–
5	–	–	0.01 μM	200 μg	–	63	37	–
6	–	–	0.01 μM	–	200 μg	55	45	–
7	0.1 mM	–	–	–	–	62	38	–
8	0.1 mM	–	0.01 μM	–	–	17	83	–
9	0.25 mM	–	–	–	–	39	61	–
10	0.25 mM	–	0.01 μM	–	–	17	83	–
11	0.1 mM	–	–	200 μg	–	35	65	–
12	0.25 mM	–	–	200 μg	–	37	63	–
13	0.1 mM	–	0.01 μM	–	–	27	73	–
14	0.25 mM	–	0.01 μM	200 μg	–	–	63	37
15	0.1 mM	–	–	–	200 μg	30	70	–
16	0.25 mM	–	–	–	200 μg	–	52	47
17	0.1 mM	–	0.01 μM	–	200 μg	–	49	51
18	0.25 mM	–	0.01 μM	–	200 μg	–	50	50
19	–	0.1 mM	–	–	–	–	79	21
20	–	0.1 mM	–	200 μg	–	–	60	31
21	–	0.1 mM	0.01 μM	200 μg	–	–	74	26
22	–	0.1 mM	–	–	200 μg	–	75	25
23	–	0.1 mM	0.01 μM	–	200 μg	–	3	4

Nck and Lin refer to the nicked and linear DNA forms respectively. In all cases SD was found to be <5%.

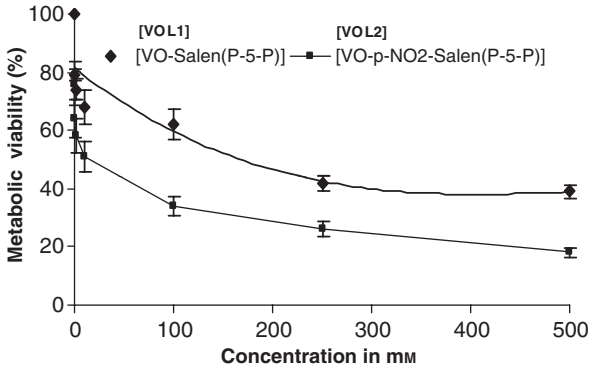

Figure 5: Cytotoxic effects of [VO-(L1)] and [VO-(L2)] in human glioma cell line (U-87 MG) studied by metabolic viability using 3-(4,5-dimethylthiazole-2-yl)-2,5-diphenyl-2H-tetrazolium bromide assay. The data points represent the mean (±SD) values.

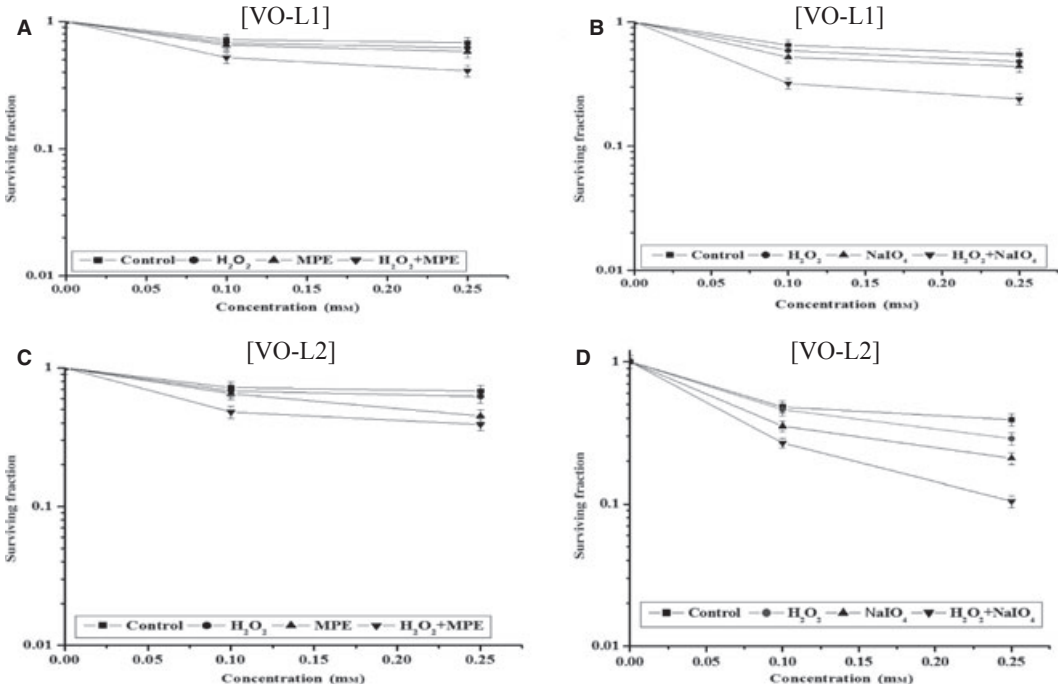

Figure 6: Cytotoxic effects of oxovanadium complexes in the presence of H_2O_2 in U-87 malignant glioma human glioma cell line determined by clonogenic survival assay (A) β-mercaptoethanol (MPE) + [VO-(L1)] (B) $NaIO_4$ + [VO-(L1)] (C) MPE + [VO-(L2)] (d)$NaIO_4$ + [VO-(L2)] in HBSS. The data points represent the mean (±SE) values.

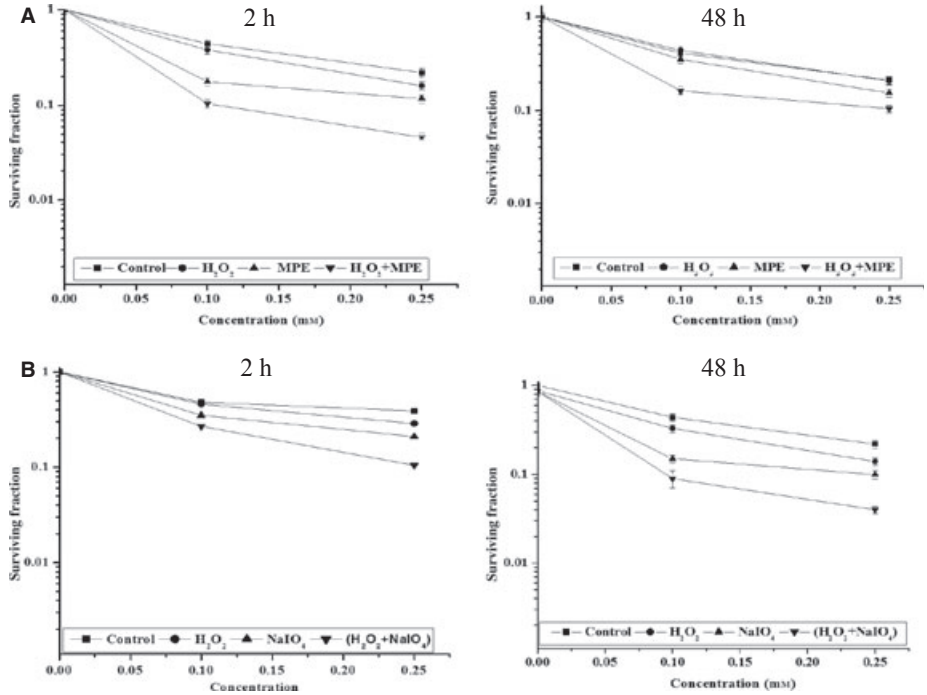

Figure 7: Cytotoxic activity of [VO-(L1)] against MDA-MB-468 human tumor cell line. Cells were incubated with increasing concentrations (0.1–0.25 mM) for 2 and 48 h (A) Effect of reducing agent [β-mercaptoethanol (MPE)]; (B) effect of oxidizing agent ($NaIO_4$) in the absence and presence of hydrogen peroxide, and the cell survival was determined by 3-(4,5-dimethylthiazole-2-yl)-2,5-diphenyl-2H-tetrazolium bromide assay. The data points represent the mean (±SE) values.

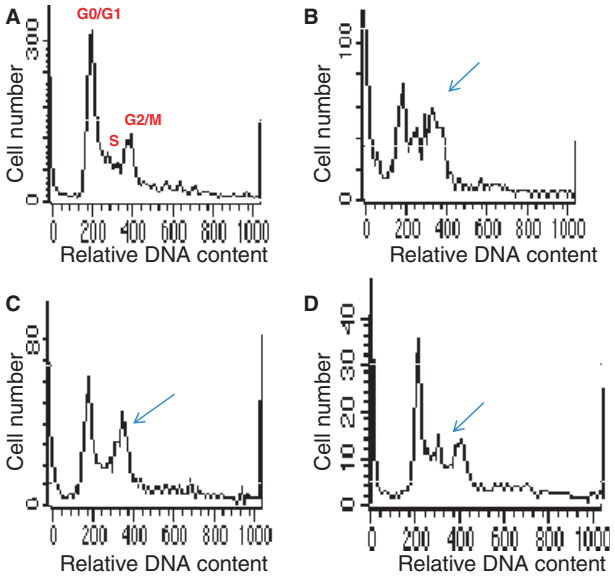

Figure 8: Effect of [VO-(L1)] on the proliferation of U-87MG cell cycle distribution (A) control, (B) 2 h (C) 24 h, (D) 48 h post-treatment.

effect with SF values more than 0.90 (Figure 6). However, when cells were treated with the complex in the presence of H_2O_2 for 2 h, the SF was significantly reduced (0.40 ± 0.06 for 0.1 mM and 0.25 ± 0.02 for 0.25 mM). The cytotoxic effect of the complex was found to be concentration dependent with SF values of 0.48 ± 0.007 and 0.39 ± 0.02 for 0.1 and 0.25 mM, respectively (Figure 6).

It is worthwhile to note that the formation of macrocolonies following exposure of 0.1 mM of vanadium complex was significantly delayed (20 against 7 days) as compared to the untreated cells, suggesting a long transient delay in the cell proliferation under these conditions.

In the presence of H_2O_2, synergistic effect was observed with reducing agent, and the SF was observed to be 0.09 ± 0.004 at 0.25 mM concentration of the complex (Figure 6). One-way ANOVA analysis was carried out to determine the significance of synergistic effect. It was found that complex with MPE in the presence of H_2O_2 was compared with control at 48 h, and the means were significantly different with $F = 40.63$ and $p = 0.003$ at 0.05 significance level.

Oxidizing agent, $NaIO_4$, was found to be more potent even at a lower concentration of the complex. Nearly 13-fold decrease in the cell survival was seen at 0.25 mM. The cytotoxic activity of the oxovanadium (IV) complexes was strongly dependent on the presence of H_2O_2 (Figure 6). Addition of the oxidizing and reducing agents significantly improves the cytotoxic activity of the oxovanadium (IV) complexes.

3-(4,5-dimethylthiazole-2-yl)-2,5-diphenyl-2H-tetrazolium bromide assay was also carried out in another cell line (breast carcinoma, MDA-MB-468) to investigate the toxicity of [VO-salen(P-5-P)]. Complex alone induced a molecular level of cytotoxicity with SF values of 0.72 ± 0.001 for a 2-h exposure and 0.68 ± 0.009 for 48 h at 0.1 mM (Figure 7) implying time-independent toxicity. With the increase in exposure time to 48 h in DMEM, a further increase in the cytotoxicity (150%) was observed. $NaIO_4$ was found to be more effective than the reducing agent with the complex. Presence of H_2O_2 further increased the toxicity by twofold as compared to the treatment with activating agent in the presence of H_2O_2 without the complex.

Cell cycle analysis

As oxovanadium compounds cause DNA breaks (Figure 4), which elicit cell cycle checkpoints response in cells, we investigated the cell cycle perturbation by flow cytometric measurements of DNA content of U-87 cells. Cells treated with 0.1 mM of the compound for 2 h at 37 °C were allowed to grow, and after removing the compounds, cells were trypsinized, fixed, stained with propidium iodide, and analyzed by flow cytometry for DNA content. The percentages of cells in each cell cycle were determined using the CellQuest Software (shown as inset in histograms). A transient delay in the progression of cells through the cell cycle (Both G1-S and G2-M transition) was induced by the complex with a near complete recovery by 48 h after removal of the complex (Figure 8).

Tumor regression analysis

To study *in vivo* effects of the complex, we investigated the growth of subcutaneous implanted EAT in mice following i.v. administration of the complex at a dose of 400 mg/kg with the time required for reaching five times the initial volume for nearly 10 days. The initial growth of tumors in untreated controls was exponential in nature (Figure 9). Administration of vanadium complex significantly delayed the growth, and the time for reaching five times the initial volume was 25 days. [VO-L1]-treated group caused a significant delay in tumor growth to be an offset from that of the untreated control which is evidenced in the peak tumor volumes of the control group occurring on day 22, whereas the same climax was reached at day 40 by the treated mice.

Discussion

We have selected pyridoxal-5-phosphate-based salen ligand described in the literature [Rocklage *et al.* (21)] as this Schiff base ligand forms highly stable coordination complexes with transition metal ions and subsequently stabilizes the aldimine Schiff base. We have synthesized oxovanadium (IV) complexes of *N,N′*-bis(pyridoxyl)-5,5′-bis(phosphate)ethylenediimine and *N,N′*-bis(pyridoxyl)-5,5′–bis (phosphate)-1″-(*p*-nitrobenzyl)ethylenediimine derivative and examined their cytotoxic activity against two different human cancer cell lines. The formation of the complexes was confirmed by IR studies.

As a part of our efforts to develop bifunctional chelating agents (BFC) (19), synthesis of new class of bifunctional Schiff base ligands and complexation with vanadium was carried out. To

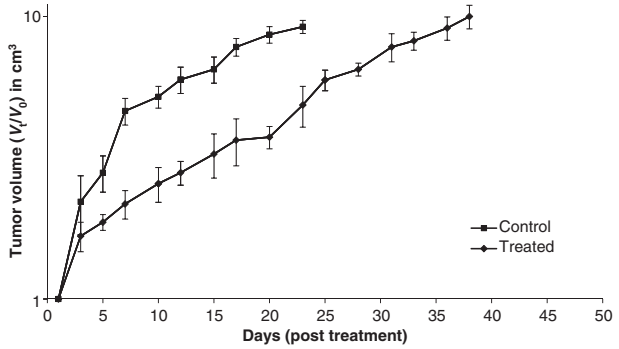

Figure 9: Effect of [VO-(L1)] on Ehrlich ascites tumor in BALB/c mice. Mean values (±SD) from 10 animals are presented.

introduce bifunctionality in the Schiff base chelating system, optically active *p*-NO_2 phenylalanine was used as a precursor to render a linking group in the system. Specificity can be generated by direct reduction of nitro group in the presence of iron powder and acetic acid by selective reduction as reported elsewhere (22) followed by conjugation of biomolecule and vanadium complexation.

The synthesized compounds are characterized on the basis of various spectroscopic techniques. IR studies of vanadium complexes confirm the formation of aliphatic –C=N– (1637 and 1639/cm for L1 and L2, respectively) with P-5-P derivatives, as well as absence of broad $–NH_2$ stretching in the range of 3200–3600/cm was observed. The IR spectra demonstrate that final compound shows sharp OH stretching band near 3400/cm, while the reactant P-5-P has broad OH stretching in the range of 3100–3400/cm at lower transmittances for phenolic compounds that disappear after complexation. EPR allows investigation of paramagnetic species of various compounds having one or more unpaired electron. Depending on the synthetic procedure, the nature and the coordination symmetries of different V(IV) species could be detected by EPR. V(IV) clusters give rise to a broad signal owing to significant dipolar interactions, whereas isolated V(IV) species exhibits hyperfine structure (HFS) derived from the interaction of free electrons (electronic configuration 3d1) with the magnetic nuclear moment of ^{51}V (I = 7/2, 99.76% of natural abundance). In the study, the EPR signal splits into eightfold lines, indicating the formation of single V(IV) species (Figure 3). For both complexes at 298 K spectrum showed isotropic nature.

As a consequence of low radius/charge ratio, vanadium(V) centers are usually strong Lewis acids, which make them suitable for the activation of peroxidic reagents (23). In the presence of excess peroxide, they are readily converted to the oxoperoxovanadium (V) complexes. In the presence of strong oxidizing agent, dominant structural unit in the coordination chemistry of vanadium in the pentavalent state is the dioxo VO^{2+} moiety, and upon addition of H_2O_2, the compounds are converted into the corresponding oxoperoxovanadium complexes that are known for their oxidizing properties (24). Investigations on the reactivity of dioxovanadium (V) complexes with H_2O_2 by Hamstra *et al.* (23) suggest that peroxide binds either to a protonated form of the vanadium complex or to the complex itself. As a weak oxidant, hydrogen peroxide can

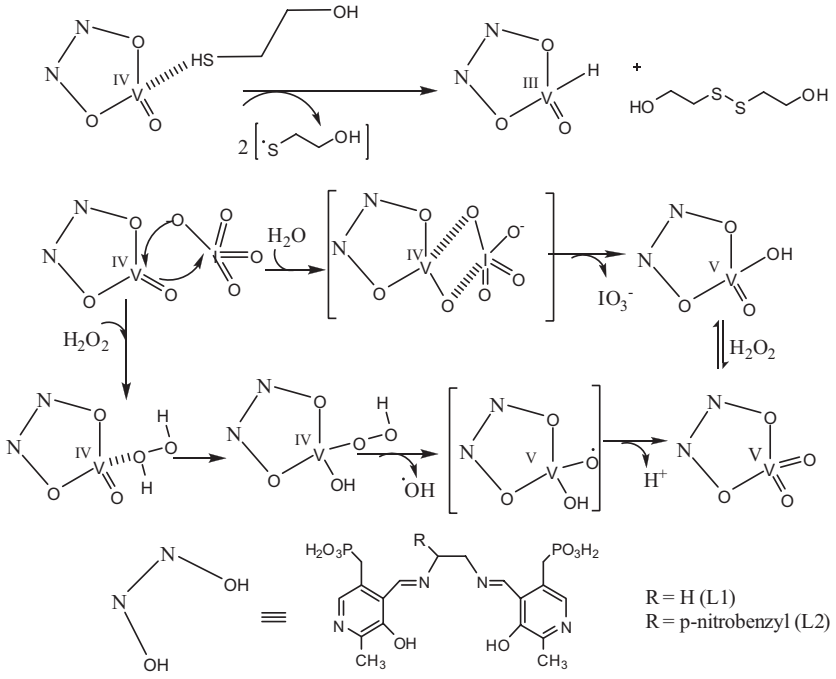

Scheme 3: Schematic representation of different oxidation states of vanadium in the presence and absence of redox agents.

lead to cellular depletion of ATP, GSH, and NADPH, as well as inducing rises in free cytosolic Ca^{2+} and activation of poly-ADP ribose polymerase, events leading to apoptosis (25). As a powerful oxidant, hydrogen peroxide decomposes *in vivo* into the extremely reactive hydroxyl radical upon reduction by metals in the cytosol or bound to lipids, proteins, and DNA. If generated at very close proximity, hydroxyl radical rapidly oxidizes these essential cellular constituents, accounting for much of the damage. In general, any drug or biological process that generates superoxide can produce hydrogen peroxide by dismutation. Hydrogen peroxide rapidly decomposes into hydroxyl radical and hydroxide anion through metal ion-catalyzed radical reactions, known as the Haber–Weiss or Fenton reaction. Proposed mechanism of different oxidation states of vanadium in the presence and absence of redox agents is given above (Scheme 3).

The sugar, the phosphate, and the base moieties constitute three chemical targets for metal-mediated reactions leading to scission of a DNA or RNA strand. Certain metal complexes, particularly those of lanthanides, can act as Lewis acids to facilitate phosphodiester hydrolysis. There are now a large number of redox-active transition metal complexes, particularly those capable of forming free or metal-bound electron-deficient oxygen species (metal-oxo, $HO^{\cdot}$, $O_2^{-\cdot}$, etc.) that trigger DNA and RNA strand scission following hydrogen atom abstraction from the ribose moiety. The heterocyclic bases like guanine in particular present a wealth of sites for metal binding and oxidation or alkylation. In principle, any metal complex that is sufficiently oxidizing to attack hydrogen atoms of the ribose moiety is also capable of abstracting an electron from G. Base oxidation does not directly yield strand scission, but rather creates a site that is sensitive to cleavage using either chemical reagents (such as HO^{-}) or enzymes, principally those involved in DNA repair.

Peroxovanadates (V) are known to generate superoxide and vanadium(IV) for DNA cleavage in the presence of additive amount of H_2O_2 (23,24) and inhibit protein-tyrosine phosphatases, the function of which is essential for mitosis progression, thereby perturbing the cell cycle progression (26) as observed here in this study also (Figure 8). The vanadium (IV)-containing compound showed substantial *in vitro* anticancer activity. This activity appears to be mediated by the reactive oxygen intermediates inducing activity of oxovanadium compounds. Although the molecular basis for the *in vitro* anticancer properties of oxovanadium (IV) compound is not completely understood at the present time, it has been shown that this type of compounds can interact with DNA and cause DNA cleavage (27). Hydroxyl radicals are generated in a pH-dependent manner in the $[VO\text{-}(L)]^{2+}H_2O_2$ system, and the optimal pH of the active species for DNA cleavage was found to be in the region between 8.5 and 9.5. The synthesized 1:1 vanadyl/Schiff base complex was found to cleave supercoiled plasmid pBR322 DNA more effectively in the presence of hydrogen peroxide (Figure 5). This DNA damaging potential appears to be partly responsible for the oxovanadium complex–induced cytotoxicity observed in human tumor cell lines which was concentration dependent (Figure 6). This notion is further supported by the observation that the presence of H_2O_2 substantially improved the cytotoxic activity.

The present study shows that oxidant and peracid are most effective in combination with the complex. Similar to clonogenic assay, the data on MTT assay show potency of oxovanadium compound on MDA-MB-468 cell line. Quantitative cytotoxicity was evident for the combination used and with the complex alone, suggesting that the redox-active compounds, [VO-(L1)] and [VO-(L2)], were able to generate oxidative stress, thereby producing cytotoxicity.

The *in vitro* results of U-87MG cells exposed to combination treatment with the complex and H_2O_2 in the presence of reducing/oxidizing agent showed an increased toxic effect (Figure 6). It therefore appears that the significant reduction in primary tumor incidence and increased delay in tumor growth were seen in the initial study. Because the majority of cancer treatments involve reducing tumor volume and prolonging life, the ability of treatment regimens to increase life spans is important.

Oxidative stress created by the reactive oxygen and other species like hydroxyl radicals damages many cellular targets besides causing DNA damage that contributes to the cell death. Damage to mitochondria not only compromises the metabolic states through fall in ATP production but also makes the cells susceptible to intrinsic pathway of apoptosis induced by a variety of signals including oxidative damage to DNA. Our *in vitro* results in both the cell lines support the proposition that the cytotoxicity of oxovanadium compounds arises on account of their oxidative stress generation ability (Figures 5–7), as both the loss of mitochondrial viability and clonogenic survival were augmented by the presence of oxidizing agents like $NaIO_4$ and H_2O_2. The *in vivo* implication of these *in vitro* observations is clearly brought out in the studies on tumor growth where a significant growth delay was noted (Figure 9), although a partial response in the form of tumor growth delay is reported here.

It is likely that under certain conditions (viz., higher dose or in combination with other agents), these complexes may in fact elicit complete response in the form of total tumor regression and cure (tumor-free survival). These initial observations are indeed encouraging to contemplate newer studies in future.

Conclusion

Our results (both *in vitro* and *in vivo*) provide experimental evidence that oxovanadium (IV) complex has the potential to be anticancer complex against human cancer cells. Redox-active vanadium (III) complexes having planar N-donor heterocyclic ligands are found to be nuclease active (28,29). Apart from antitumor activity, we have developed cell homing peptides conjugated to the developed system and evaluated that the complexes activate glycogen synthesis in rat adipocytes. Thus, the development of these vanadium compounds holds promise for explosion of novel antitumor/antidiabetic agents by enhancing the positive effects of vanadium as an oral therapeutic adjunct in diabetic control, while minimizing potential toxicity. It is our further aim to optimize VO-L1 and VO-L2 and conjugate antisense oligonucleotide, which may provide the basis for the design of potentially effective target-specific complex for the treatment of cancer.

Acknowledgments

We thank Dr R. P. Tripathi, Director INMAS, for providing necessary facilities. The work was supported by Defence Research and Development Organization, Ministry of Defence, under R&D project INM–311 and Indian Council for Medical Research under project 45/3/2006/PHA/BMS.

Declaration of Interest

The authors report no conflicts of interest. The authors alone are responsible for the content and writing of the paper.

References

1. Rehder D. (1991) The bioinorganic chemistry of vanadium. Angew Chem Int Ed Engl;30:148–167.
2. Butler A., Carrano C.J. (1991) Coordination chemistry of vanadium in biological systems. Chem Rev;109:61–105.
3. Larrow J.F., Jacobsen E.N. (2004) Asymmetric processes catalyzed by Chiral (Salen) metal complexes. Top Organo Chem;6:123–152.
4. El-Naggar M.M., El-Waseef A.M., El-Halafawy K.M., El-Sayed I.H. (1998) Antitumor activities of vanadium(IV), manganese(IV), iron(III), cobalt(II) and copper(II) complexes of 2-methylaminopyridine. Can Lett;133:71–76.
5. Kulkarni A.K., Patil A.S., Badami P.S. (2009) Synthesis, characterization, DNA cleavage and *in vitro* antimicrobial studies of La(III), Th(IV) and VO(IV) complexes with Schiff bases of coumarin derivatives. Eur J Med Chem;44:2904–2912.
6. Chohan Z.H., Sumrra S.H., Youssoufi M.H., Hadda T.B. (2010) Metal based biologically active compounds: design, synthesis, and antibacterial/antifungal/cytotoxic properties of triazole-derived Schiff bases and their oxovanadium(IV) complexes. Eur J Med Chem;45:2739–2747.
7. Hirao T. (1997) Vanadium in synthesis modern organic. Rev Chem;97:2707–2724.
8. Colpas G.J., Hamstra B., Kampf J., Pecoraro V.L. (1994) The preparation of VO3+ and VO2+ complexes using hydrolytically stable, asymmetric ligands derived from Schiff base precursors. Inorg Chem;33:4669.
9. Kostova I. (2009) Titanium and vanadium complexes as anticancer agents. Med Chem;9:827–842.
10. Evangelou A.M. (2002) Vanadium in cancer treatment. Crit Rev Oncol Hematol;42:249–265.
11. Bishayee A., Waghray A., Patel M.A., Chatterjee M. (2010) Vanadium in the detection, prevention and treatment of cancer: the *in vivo* evidence. Cancer Lett;294:1–12.
12. Djordjevic C. (1995) Antitumor activity of vanadium compounds. In: Sigel H., Sigel A., editors. Metal Ions in Biological Systems. New York: Marcel Dekker Publisher; p. 595–616.
13. Kwong D.W., Chan O.Y., Wong R.N., Musser S.M., Vaca L., Chan S.I. (1997) DNA-photocleavage activities of vanadium(V) – peroxo complexe. Inorg Chem;36:1276–1277.
14. Byczkowski J.Z., Wan B., Kulkarni A.P. (1988) Vanadium-mediated lipid peroxidation in microsomes from human term placenta. Bull Environ Contam Toxicol;41:696–703.
15. Sakurai H., Tamura H., Okatami K. (1995) Mechanism for a new antitumor vanadium complex: hydroxyl radical-dependent DNA cleavage by 1,10-phenanthroline vanadyl complex in the presence of hydrogen peroxide. Biochem Biophys Res Commun;206:133–137.
16. Keller R.J., Sharma R.P., Grover T.A., Piette L.H. (1988) Vanadium and lipid peroxidation: evidence for involvement of vanadyl and hydroxyl radical. Archiv Biochem Biophys;265:524–533.
17. Ozawa T., Hanaki A. (1989) ESR evidence for the formation of hydroxyl radicals during the reaction of vanadyl ions with hydrogen peroxide. Chem Pharm Bull;37:1407–1409.
18. Richardson D.R., Milnes K. (1997) The potential of iron chelators of the pyridoxal isonicotinoyl hydrazone class as effective antiproliferative agents II: the mechanism of action of ligands derived from salicylaldehyde benzoyl hydrazone and 2-hydroxy-1-naphthylaldehyde benzoyl hydrazone. Blood;89:3025–3038.
19. Mishra A.K., Panwar P., Chopra M., Sharma R.K., Chatal J.F. (2003) Synthesis of novel bifunctional Schiff-base ligands derived from condensation of 1-(*p*-nitrobenzyl)ethylenediamine and 2-(*p*-nitrobenzyl)-3-monooxo-1,4,7-triazaheptane with salicylaldehyde. New J Chem;27:1054–1058.
20. Verquin G., Fontaine G., Bria M., Zhilinskaya E., Abi-Aad E., Aboukaıs A., Baldeyrou B., Bailly C., Bernie J. (2004) DNA modification by oxovanadium(IV) complexes of salen derivative. J Biol Inorg Chem;9:345–353.
21. Rocklage S.M., Cacheris W.P., Quay S.C., Hahn F.E., Raymond K.N. (1989) Manganese(II) *N,N'*-dipyridoxylethylenediamine-*N,N'*-diacetate 5,5′-bis(phosphate). Synthesis and characterization of a paramagnetic chelate for magnetic resonance imaging enhancement. Inorg Chem;28:477–485.
22. Laso N.M., Quiclet-Sire B., Zard S.Z. (1996) A new selective reduction of nitroalkenes into enamides. Tetrahedron Lett;37:1605–1608.
23. Hamstra B.J., Colpas G.J., Vincent P.L. (1998) Reactivity of dioxovanadium(V) complexes with hydrogen peroxide: implications for Vanadium Haloperoxidase. Inorg Chem;37:949–995.
24. Shul'pin G.B. (2002) Metal-catalyzed hydrocarbon oxygenations in solutions: the dramatic role of additives: a review. J Mol Catal A: Chemical;189:39–66.
25. Sauerheber R.D., Cochrane C.G. (1988) Mechanisms of oxidant-mediated cell injury. The glycolytic and mitochondrial pathways of ADP phosphorylation are major intracellular targets inactivated by hydrogen peroxide. J Biol Chem;263:1665–1675.
26. Narla R.K., Dong Y., D'Cruz O.J., Navara C., Uckun F.M. (2000) Bis(4,7-dimethyl-1,10-phenanthroline) sulfatooxovanadium(IV) as a novel apoptosis-inducing anticancer agent. Clin Cancer Res;6:1546–1556.
27. Sasmal P.K., Patra A.K., Chakravarty A.R. (2008) Synthesis, structure, DNA binding and DNA cleavage activity of oxovanadium(IV) *N*-salicylidene-S-methyldithiocarbazate complexes of phenanthroline bases. J Inorg Biochem;102:1463–1472.
28. Niedwieski A.C., Hitchcock P.B., Neto J.D.D.M., Wypych F., Leigh G.J., Nunes F.S. (2003) Vanadium(II)-diamine complexes: synthesis, UV-Visible, infrared, thermogravimetry, magnetochemistry and INDO/S characterisation. J Braz Chem Soc;14:750–758.
29. Bond M.R., Czernuszewicz R.S., Dave B.C., Mohan M., Verastgue R., Carrano C.J. (1995) Spectroscopic and magnetostructural correlations in oxo-bridged dinuclear vanadium(III) complexes of potential biological significance. Inorg Chem;34:5857–5869.

Supporting Information

Additional Supporting Information may be found in the online version of this article:

Figure S1. Mass spectrum of *N,N′*-bispyridoxyl-5, 5′–bis (phosphate) ethylenediimine (L1).

Figure S2. ^{31}P-NMR of Oxovanadium (IV) complex of *N,N′*-bispyridoxyl-5, 5′–bis (phosphate) ethylenediimine [VO-L1].

Figure S3. Mass spectrum of *p*-nitrobenzylethylenediamine (**2a**).

Figure S4. Mass spectrum of *N,N′*-bis(pyridoxyl)-5,5′-bis(phosphate)-1″-(*p*-nitrobenzyl)ethylenediimine (L2).

Please note: Wiley-Blackwell is not responsible for the content or functionality of any supporting materials supplied by the authors. Any queries (other than missing material) should be directed to the corresponding author for the article.